Michigan Institute for Plasma Science and Engineering (MIPSE)

1ST ANNUAL GRADUATE STUDENT SYMPOSIUM

September 29, 2010

3:00 – 7:00 pm

1200 EECS, 1301 Beal Avenue

North Campus

University of Michigan
Ann Arbor, MI

MIPSE 1st Graduate Student Symposium

Schedule

3:00 – 5:00	**Plenary Session** **Chair:** Prof. Mark J. Kushner (Director, MIPSE)
3:00 – 3:10	Prof. David C. Munson (Dean, College of Engineering) ***Opening Remarks***
3:10 – 4:00	Dr. Bruce A. Remington (Lawrence Livermore National Laboratory) ***From High Energy Density Laboratory Astrophysics to Extreme Materials Science: Pushing the Frontiers of Experimental Science***
	Student Talks
4:00 – 4:15	Christopher McGuffey ***Compact High-Brilliance Synchrotron Source Driven by a Tabletop Laser***
4:15 – 4:30	Tiberius Moran-Lopez ***The Modeling of Turbulent Radiative Shocks with Applications to High Energy Density Physics and Astrophysics***
4:30 – 4:45	Brian Peterson ***High-Speed Flow and Fuel Imaging study of Available Spark Energy in a Spray-Guided Direct Injection Engine and Implication on Misfires***
4:45 – 5:00	Bradley Sommers ***An Investigation of Harmonically Driven Bubbles in a Wire-Plane Electrode Geometry***
5:00 – 5:15	**Break (refreshments will be served)**

5:15 – 5:45 **Poster Session I**

Iverson Bell
Electrodynamic Tethers for ChipSats and Nanospacecrafts

Julie Feldt
GITM Synthetic TEC Comparison with GPS Data

David Liaw
Simulation of Self-Neutralization Techniques for Charged Particle Thrusters on Nanospacecraft

Rohit Shastry
Erosion Characterization via Ion Power Deposition Measurements in a 6-kW Hall Thruster

Calvin Zulick
K-Shell Spectroscopy of Au Plasma Generated with a Short Pulse Laser

Will Schumaker
Betatron X-ray Spectra from a Laser Wakefield Accelerator Using Ionization Injection

Pooya Movahed
Multi-Layered Richtmyer-Meshkov Instability

Zhaohan He
A High-Repetition Rate LWFA for Studies of Laser Propagation and Electron Generation

Franklin Dollar
Narrow Energy Spread Proton and Ion Spectra from High-Intensity Laser Interactions

5:45 – 6:15 **Poster Session II**

Paul Cummings
A Computational Investigation of the Impact of Non-Gaussian, "Low-Quality" Laser Pulses on Electron Beam Properties in Laser-Wakefield Acceleration Experiments

Channing Huntington
Radiative Stabilization of Rayleigh-Taylor Instabilities in Supernova-Relevant Experiments on the National Ignition Facility

Angela Dixon
Guided Corona Generates Wettability Patterns That Selectively Direct Cell Attachment inside Closed Microchannels

Matthew Franzi
Recirculating Planar Magnetrons: Simulations and Experiment

David French
Electron Dynamics in Crossed Field Devices

Eric Gillman
Cathode Spot Ejected Particle Image Velocimetry (PIV) Calculations

Matthew Gomez
Investigation of Plasma Formation and Evolution in Post-Hole Convolutes

Aimee Hubble
Spatially Resolved Study of Inter-Cusp Transport and Containment of Primary Electrons

Robert Lobbia
Time-Resolved Electron Energy Distribution Functions: Preliminary Results and Development of a Rapidly Swept Langmuir Probe System

Michael Logue
Modeling Reaction Rates in Ar/N_2 ICP Plasmas Using Pulsed Power for a Variety of Duty Cycles, Pressures, Average Powers, and Frequencies

Juline Shoeb
Fluorocarbon Polymer Removal in H_2/He Plasmas with NH_3 Plasma Sealing of Porous Low-k Dielectric

6:15 – 6:45 **Poster Session III**

Sang-Heon Song
Control of Electron Energy Distributions and Flux Ratio in Pulsed Capacitively Coupled Plasmas with Different Duty Cycle and Pulse Repetition Frequency

Sameh Tawfick
Fabrication of 3D Carbon Nanotube Microstructures by Capillary Forming

Wei Tian
Different Patterns of High-Energy and Low-Energy Electrons in an Atmospheric-Pressure Microplasma Generated by a Hairpin Resonator

Jun-Chieh Wang
Electron Current Extraction from RF Excited Micro-Dielectric Barrier Discharges

Benjamin Yee
New Diagnostic Capabilities for NASA's Pulsed Nanosecond Discharge

Peng Zhang
Evaluation of RF Power Absorption and Electric and Magnetic Field Enhancements Due to Surface Roughness

Peng Zhang
Electrical Contact Resistance with Dissimilar Materials

Cyril Galitzine
Simulation of the Interaction between Two Rarefied Ionized Jets Using a Hybrid Method

Laura Spencer
Experimental and Computational Study of Carbon Dioxide Dissociation in an Atmospheric Pressure Microwave Discharge

6:45 – 7:00 **Best Presentation Award**

ABSTRACTS

Michigan Institute for Plasma Science and Engineering Seminar

From High Energy Density Laboratory Astrophysics to Extreme Materials Science: Pushing the Frontiers of Experimental Science

Dr. Bruce A. Remington
Lawrence Livermore National Laboratory

Wednesday, 29 September 2010 - 3:00 pm
Room 1200 EECS Building

Abstract

Modern high power lasers and magnetic pinch facilities ("Z pinches") have opened up a new class of experimental science, generically called high energy density physics (HEDP). The range of HED science currently under investigation or planned is very broad. Examples include the study of supernova explosion hydrodynamics; collisionless shocks in interstellar space; relativistic electron-positron pair plasmas; gamma-ray burst dynamics; x-ray photoionized plasmas in accreting black holes; planetary physics; and material dynamics under extreme conditions. I will describe several examples from this new class of experimental science, and suggest some interesting possibilities for the future.

About the Speaker: **Bruce Remington has been a staff physicist at LLNL in the Inertial Confinement Fusion (ICF) Program since 1988, and a Group Leader since 1996. He and his group work on laser driven, high energy density (HED) fluid instabilities, HED laboratory astrophysics, and solid-state dynamics at high pressures and strain rates. He received his BS degree from Northern Michigan University in 1975 and his PhD degree in nuclear physics from Michigan State University in 1986. He is a recipient of the APS-DPP Excellence in Plasma Physics Award for his work on ablation-front Rayleigh-Taylor instabilities, and he is a Fellow of the American Physical Society.**

Abstracts - Oral Presentations

Compact High-brilliance Synchrotron Source Driven by a Tabletop Laser

C. McGuffey [a], W. Schumaker [a], S. Kneip [b], F. Dollar [a], A. Maksimchuk [a], A. G. R. Thomas [a], and K. Krushelnick [a]

(a) University of Michigan, Center for Ultrafast Optical Science (cmcguffe@umich.edu)
(b) Imperial College, London (stefan.kneip@gmail.com)

Numerous fields of the scientific community have found applications of x-rays such as biological or material imaging. To satiate this demand, countries worldwide have created large user facilities based on radio-frequency accelerators, and built new generations of these facilites as new technologies became available. Currently, facilities are being built or upgraded to fourth generation technologies, with price tags in the hundreds of millions of dollars. These fourth generation facilities intend to produce high repetition rate ~keV x-ray pulses with ~100 fs duration. This pulse duration approaches the time resolution required to observe molecular and atomic dynamics. This presentation reports on the demonstration of a compact high spectral brilliance x-ray source driven by an ultrafast tabletop laser. This source could make keV x-ray radiography available to university-scale research.

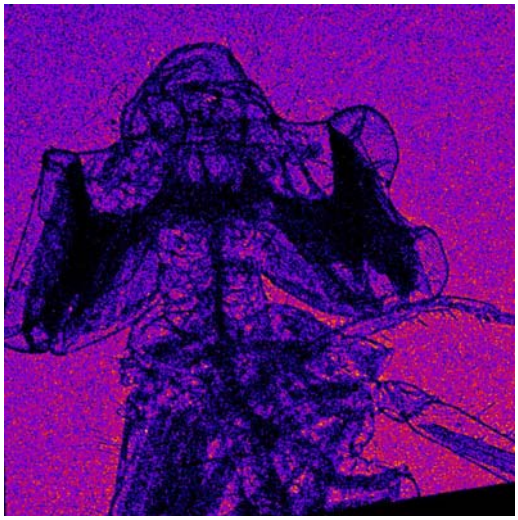

Fig. 1: Single shot x-ray radiograph of the head of a damselfly. Note that the fine hairs are resolved, internal structures are revealed, and boundaries are sharply defined- this is phase contrast imaging due to partial spatial coherence of the source.

The Hercules laser at the University of Michigan is a leading facility for studies of laser driven particle acceleration. Hercules's high power (100 TW) and ultrashort pulse duration (30 fs) make it well-suited for studies of laser wakefield acceleration (LWFA) [1]. LWFA takes place when a high intensity laser propagates through an underdense plasma and the ponderomotive force of the laser drives a plasma wave. Electrons injected at the proper phase of this wave can gain relativistic energies (up to 600 MeV with Hercules).

Electron beams produced by LWFA have been attractive as drivers in conventional wiggler synchrotron sources. However, it turns out that the structure of the plasma wakefield itself is an ideal wiggler, with dimensions on the order of the plasma wavelength (10s of μm). This microscopic scale means that synchrotron radiation produced as beam electrons wiggle in the wake will have wavelength in the x-ray or even gamma ray range. The x-rays have been characterized in two experimental campaigns [2]. The divergence, source size, spectrum, and coherence were measured. The high degree of collimation and plentiful photon yield result in an x-ray beam which has peak spectral brilliance greater than most third generation synchrotron facilities, greater energy (10s of keV), and presumably with duration ≤ 10 fs.

References

[1] T. Tajima and J. M. Dawson, Phys. Rev. Lett. **43**, 267-270 (1979).
[2] S. Kneip, C. McGuffey, J. L. Martins, et al., Submitted to Nature Physics (2010).

The Modeling of Turbulent Radiative Shocks with Applications to High Energy Density Physics and Astrophysics

Tiberius Moran-Lopez [a], James P. Holloway [a] and Oleg Schilling [b]

(a) University of Michigan (timoran@umich.edu, hagar@umich.edu)
(b) Lawrence Livermore National Laboratory (schilling1@llnl.gov)

Radiation transport, shock physics, and turbulence are coupled in many high energy density environments including supernova explosions and stellar life cycles in the interstellar media, high-energy laser experiments, Z-pinches, and black hole interactions with molecular clouds and binary stars. A turbulent radiation hydrodynamics model that can be used to examine such phenomena is developed in this work. A four-equation Reynolds-averaged Navier–Stokes model for the turbulent kinetic energy, turbulent kinetic energy dissipation rate, density variance, and temperature variance is used to describe the effects of turbulence while an equilibrium diffusion model (where radiation and material temperature are in thermal equilibrium) describes the radiative transfer. Gradient-diffusion and similarity closure approximations are generalized to account for radiative effects. The mean radiative flux introduces additional terms requiring closure approximations addressed by modeled transport equations for the temperature and density variance. A simplified model can be obtained by assuming that the radiation energy density and opacity are uncorrelated. The Rankine–Hugoniot relations for the turbulent equilibrium diffusion model are also derived to obtain post-shock velocity and total pressure relations; these reduce to the classical relations when radiation and turbulence are neglected. This model will contribute to an improved understanding of high energy density and astrophysical phenomena in which radiation and turbulence are important.

This work was funded by the U. S. Department of Energy NNSA under the Predictive Science Academic Alliances Program by grant DE-FC52-08NA28616 and performed under the auspices of the DOE by Lawrence Livermore National Laboratory under Contract DE-AC52-07NA27344.

High-Speed Flow and Fuel Imaging Study of Available Spark Energy in a Spray-Guided Direct Injection Engine and Implication on Misfires

Brian Peterson [a], David L. Reuss [a] and Volker Sick [a,b]

(a) Department of Mechanical Engineering, University of Michigan
2026 W. E. Lay Automotive Laboratory, 1231 Beal Ave., Ann Arbor, MI 48109-2133 USA
(bpete@umich.edu)
(b) Center of Smart Interfaces, Petersenstraße 32
64287 Darmstadt, Germany

Spark energy transferred under the highly stratified conditions during late injection in a spray-guided spark-ignition direct-injection (SG-SIDI) engine is not well characterized. The impact of high pressures, temperatures, velocities, and variations in local fuel concentration along with temporal and/or spatial variations on spark performance must be better characterized. Therefore, high-speed particle image velocimetry (PIV) experiments are conducted to characterize the spark energy dependence for a wide range of well-defined homogeneous fuel-air equivalence ratios ($\Phi = 0 – 2.9$) and air velocities (0 – 12 m/s) in an optical SG-SIDI engine.

Results from the well-defined operating conditions are used to interpret spark events under late injection, stratified operation in the SG-SIDI engine. For this investigation, high-speed particle image velocimetry (PIV), high-speed planar laser-induced fluorescence (PLIF) imaging, and spark-discharge electrical measurements are used to obtain flow field, fuel concentration, and spark discharge measurements. Measurements of velocity magnitude, shear strain rate magnitude, vorticity magnitude, and normalized fuel concentration are extracted in a 4 x 4 mm region directly downstream of the spark plug at the time of spark to characterize the in-cylinder conditions near the spark plasma at the time of spark. Correlations between spark energy and measurements of velocity, shear strain rate, vorticity, and equivalence ratio are examined to investigate rare ignition instability events among predominately well-burning engine cycles.

An Investigation of Harmonically Driven Bubbles in a Wire-Plane Electrode Geometry

Bradley S. Sommers [a], John E. Foster [b]

(a) Dept. of Nuclear Engineering, University of Michigan,USA (bsso@umich.edu)
(b) Dept. of Nuclear Engineering, University of Michigan,USA (jefoster@umich.edu)

Electrical forces acting on bubbles in water arise from the dielectric properties of the bubble-liquid interface and the free charge deposited there by the water's conductivity. This electrical stress can cause strong distortion of the bubble's size and shape, which is well documented for the case of a D.C. field [1]. In this work, we investigate the effects of a time dependent A.C. field on the bubble's shape, particularly by matching the applied field frequency to the bubble's natural oscillating frequency, which is governed by the bubble's surface tension and internal pressure [2]. By driving the bubble into such resonant motion, it may be possible to significantly change the bubble's internal pressure and charge polarization, thereby leading to changes in the conditions for plasma breakdown. A better understanding of such effects could be used to facilitate the process of plasma breakdown in water.

Figure 1. Plasma breakdown along the internal surface of the bubble.

An outline of the experimental setup is shown in Figure 2. An air pump is used to launch bubbles into a glass tube, filled with distilled water, where they pass between electrodes arranged in a wire-plane geometry. An electric field is applied between the electrodes by a 500 Watt A.C. power supply stepped up by a 20 kV transformer. Bubbles are driven by A.C. signals in the range 50-1000 Hz and the response is investigated using a high speed camera (10,000 frames per second), oscilloscope, and spectrometer.

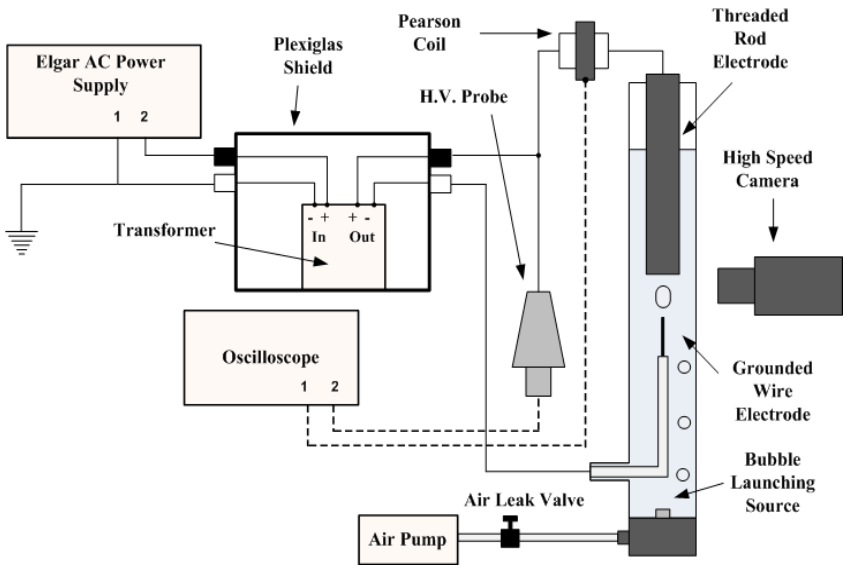

Figure 2. The experimental setup employed to study bubble deformation under the action of an electric field.

References

[1] Garton, C.G., Krasucki, C.G., *Bubbles in insulating liquids: stability in an electric field*, Proc. Royal Soc. Lon., Vol. **280**, No. 1381, July 21, 1964.
[2] Brennen, C.E., *Cavitation and Bubble Dynamics*, New York, Oxford University Press, 1995.

Abstracts – Poster Session I

Electrodynamic Tethers for ChipSats and Nanospacecrafts

Iverson Bell, III [a], Brian Gilchrist [a], Sven Bilén [b], Robert Hoyt [c], Nestor Voronka [c]

a) The University of Michigan, Ann Arbor, MI 48109
(Icbell@umich.edu, Gilchrst@umich.edu)
b) The Pennsylvania State University, University Park, PA 16802 (SBilen@engr.psu.edu)
c) Tethers Unlimited, Inc. 11711 N. Creek Pkwy S., Bothell WA 98011
(Hoyt@tethers.com, Voronka@tethers.com)

The recent interest in Nanospacecraft (1-10 kg) over the past decade has spawned an interest to assess even smaller spacecraft. Based on integrated circuit technology, the potential of highly miniaturized spacecraft at the levels of hybrid integrated circuits and fully monolithic computer chips is being investigated. These small "chip" satellites, or ChipSats, would have the potential of leveraging the technology development of highly integrated, highly capable microelectromechanical systems (MEMS) and could be substantially less expensive to bring into orbit. ChipSats are thus a new generation of lightweight (on the order of grams and milligrams), small spacecraft that can be released in swarms, for example, to provide a unique form of data collection. Early ChipSat concepts have no propellant and a low ballistic coefficient, which is typically less than 1, so ChipSats maintain their orbit for no more than a few days in low Earth orbit. We are asking the question if a very short electrodynamic tether system, or EDT, (flexible or semi-rigid) can be used to meet the challenge of maintaining ChipSat orbit and harvesting energy without contributing significantly to the ChipSat mass, required onboard power, or atmospheric drag relative to the thrust. Most previous EDT work accounts for tethers that are kilometers long. The results from this work provide insight into the physics of very short EDTs and smaller structures in space.

The electrodynamic tether, a conductor traveling through the earth's magnetic field, exploits the Lorentz force to generate an intrinsic electromotive force along its axis of orbital motion. Current flows along the EDT because it is a low-resistance path connecting different regions of the ionosphere. As a result, the EDT provides spacecrafts orbiting Earth (or other bodies with a magnetic field) with a means of either converting kinetic energy into electrical power or using the spacecraft's power to generate upward or downward thrust without consumables. We discuss the practical trade-offs regarding drag, mass, tether and collector material, emitter type, and power when designing EDTs for such small and lightweight system. These characteristics will be examined to determine how they affect the orbital maintenance of the ChipSat. Furthermore, we use EDT simulation software to calculate tether voltages and induced currents based on tether configuration, mission parameters, and ambient conditions.

GITM Synthetic TEC Comparison with GPS data

Julie A. Feldt and Mark Moldwin

Department of Atmospheric, Oceanic, and Space Sciences, University of Michigan, 2455 Hayward St., Ann Arbor, MI 48105 (jfeldt@umich.edu, mmoldwin@umich.edu)

Since the ionosphere is the interface between the Earth and space environments and impacts radio, television and satellite communication, it is imperative to model and predict it well. The ionosphere undergoes changes due to plasma transport, chemistry and impact ionization during geomagnetic storms and intervals where energy, mass and momentum are rapidly transferred from the solar wind to the Earth's space environment. Ionospheric changes can cause scintillation in Global Positioning System (GPS) signals, and interruption in satellite communication. Geomagnetic storms also generate changes in the plasmasphere and therefore impact the radiation belts and the ring current. Unless ionospheric and plasmaspheric dynamics can be detected and predicted, space weather problems will impact society with regards to communication and space travel.

At the University of Michigan, Aaron Ridley created the Global Ionosphere-Thermosphere Model (GITM) to contribute to the Space Weather Modeling Framework, whose goal is to model from Sun to the mud. GITM is a physics-based and partially empirical, 3-D spherical model of the Earth's thermosphere and ionosphere system using a stretched grid in latitude and altitude. GITM reproduces the ionosphere and thermosphere from 90 to 500km, therefore covering the main ionospheric electron density peak, but not the topside ionosphere or plasmasphere (which could also boost electron density).

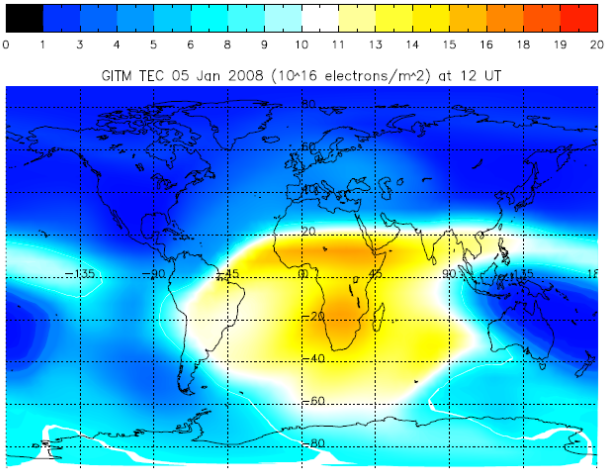

Fig. 1: A GITM Global TEC observation where the color indicates the magnitude of TEC. Note that the highest values of TEC are at noon local time and near the equator.

A good determination of an effective ionospheric model is looking at how well the electron distribution matches with data. One way of doing this is to look at the total electron content (TEC). TEC is the column density of electrons between two points within an area of one meter squared, which gives an altitude integrated simulative model of the electron density variation over the entire globe. Fig. 1 shows a TEC extraction from GITM during quiet time. In this study GITM is compared to GPS TEC data to determine the effects of the topside ionosphere and plasmasphere on TEC values and to test the accuracy of the model.

Simulation of Self-Neutralization Techniques for Charged Particle Thrusters on Nanospacecraft

David Liaw, Brian Gilchrist

University of Michigan, Ann Arbor, MI 48109

There is an emerging class of nanospacecraft thrusters that use colloids or nanoparticles that can be charged either positively or negatively to provide thrust. An issue to be examined is how the ability to charge particles to either polarity is beneficial to the system in terms of being able to provide self-neutralization of the thruster. Here, we focus on the capabilities of the nanoparticle field extraction thruster (NanoFET) to self-neutralize (although it applies to colloidal systems as well). The NanoFET system operates by expelling either positively or negatively charged nanoparticles through a gridded structure. This ability to charge nanoparticles to either polarity offers the flexibility to also use the nanoparticles to neutralize the system. Most common electric propulsion systems only emit positively-charged ions, which requires that electrons are also emitted, often through the use of hollow cathodes or other electron emitters. These neutralization techniques all reduce efficiency. If NanoFET were able to use oppositely charged nanoparticles to self-neutralize, there would be no loss of efficiency due to the neutralization process.

We explore two approaches for charged particle thruster neutralization: spatially and temporally separated oppositely charged populations of nanoparticles. Both solutions would result in equal amounts of both charged populations being emitted, resulting in a charge neutral spacecraft. If NanoFET were to operate without a neutralization technique, it would result in the spacecraft charging up. This would eventually result in the emitted particles returning to the spacecraft, which would adversely affect thrust.

The spatially separated approach requires different emission regions each of which emits particles of a single polarity. Even though each region will only be emitting particles of a single polarity, the net emitted charge of all the regions would be zero. How the beams of opposite charge will interact once emitted are explored through analysis and simulation.

The temporally varying approach requires emission of oppositely charged particles out of a single region in AC operation. Over time, the net emitted charge of the region will be zero. The issues that are addressed will be how charging of the spacecraft over short time intervals affect the emitted beam, and how the oppositely charged beam "packets" will interact once emitted.

We simulate the adverse effects of no neutralization technique, as well as both neutralization techniques through XOOPIC, an object oriented particle in cell simulation tool in 2.5 dimensions. We also optimize the neutralization techniques and examine the feasibility of such methods.

Erosion Characterization via Ion Power Deposition Measurements in a 6-kW Hall Thruster

Rohit Shastry [a], Alec D. Gallimore [a] and Richard R. Hofer [b]

(a) The University of Michigan, Ann Arbor, MI 48109 (rshastry@umich.edu, alec.gallimore@umich.edu)

(b) Jet Propulsion Laboratory (Richard.R.Hofer@jpl.nasa.gov)

Hall thruster lifetime models currently in development aim to provide predictive tools that would eliminate or substantially reduce the need to perform long-duration, expensive life tests of flight articles. A critical part of these modeling efforts is the need to understand and characterize the interaction between the plasma and the discharge channel walls. In particular, measurements of ion current and power incident on the ceramic walls would greatly contribute to the understanding of Hall thruster sheath physics, as well as provide validation and/or allow refinement of existing sheath models. To this end, incident ion power deposition was measured along the inner and outer channel walls of a 6-kW laboratory Hall thruster [1]. Five Langmuir probes were flush-mounted onto each erosion ring of the thruster, spanning 0.02 – 0.14 channel lengths from the exit plane. Data were taken over eight operating conditions ranging from 150 to 400 V discharge voltage and roughly 1.3 to 6 kW discharge power. The incident ion power deposition density and angle of ions were determined at each probe location, and used to characterize the erosion as a function of discharge voltage and power. It was found that overall power deposition increased with discharge voltage and anode mass flow rate, except at voltages lower than 200 V. At these voltages, the ion flux to the walls was found to be higher than expected, leading to increased power deposition densities. This trend has been attributed to a larger beam divergence at low voltage operation, which has been confirmed with near-field ion current density measurements [2]. These data provide an excellent basis for comparison against and refinement of existing sheath models for Hall thruster lifetime predictions.

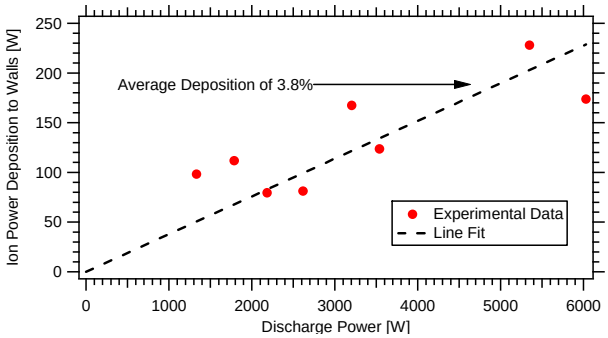

Figure 1: Measured ion power deposition to inner and outer channel walls as a function of discharge power.

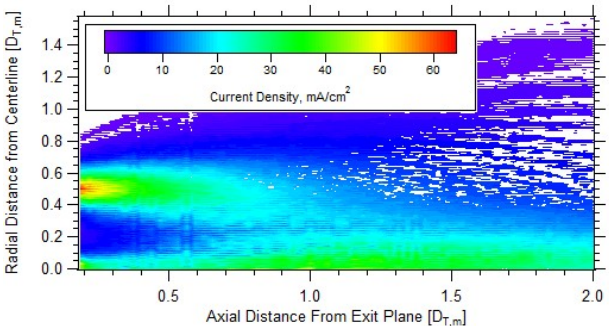

Figure 2: Ion current density map in the near-field plume used to calculate divergence.

References

[1] Shastry, R., Gallimore, A. D., and Hofer, R. R., "Erosion Characterization via Ion Power Deposition Measurements in a 6-kW Hall Thruster," Presented at the 57th JANNAF Propulsion Meeting, JANNAF-2010-1205, Colorado Springs, CO, May 3 - 7, 2010.

[2] Reid, B. M. and Gallimore, A., "Near-field Ion Current Density Measurements of a 6-kW Hall Thruster," Presented at the 31st International Electric Propulsion Conference, IEPC-2009-124, Ann Arbor, MI, September 20 - 24, 2009.

K-Shell Spectroscopy of Au Plasma Generated with a Short Pulse Laser

Calvin Zulick [a], Franklin Dollar [a], Hui Chen [b], Katerina Falk [c], Andy Hazi [b], Chris Murhpy [c], Jaebum Park [b], John Seely [d], Ronnie Shepherd [b], Csilla Szabo-Foster [d], Riccardo Tommasini [b]

(a) Center for Ultrafast Optical Science, University of Michigan (czulick@umich.edu)
(b) Lawrence Livermore National Laboratory, L-472
(c) Clarendon Laboratory, University of Oxford
(d) Space Science Division, Naval Research Laboratory

The production of x-rays from electron transitions into K-shell vacancies (K-α/β emission) is a well known process in atomic physics and has been extensively studied as a plasma diagnostic in low and mid Z materials[1-2]. Such spectra from near neutral high-Z ions are very complex and therefore difficult to describe with atomic calculations. In this experiment a high Z (gold) plasma was created with a short pulse laser producing a complex non-local thermodynamic equilibrium (non-LTE) plasma. A transparent bent quartz crystal spectrometer with a hard x-ray energy window, ranging from 17 to 102 keV, was used to measure the emission spectrum. The Titan laser system at Lawrence Livermore National Laboratory was used to deliver an approximately 350 joule laser pulse, with a 10 picosecond duration and a wavelength of 1054 nm, to the Au target.

K-$\alpha_{1,2}$ and K-$\beta_{1,2,3}$ transitions were observed over a range of target sizes. Additionally, a series of shots was conducted with a pre-ionizing long pulse (3 nanosecond, 1-10 joule, 527 nanometer) on the backside of the target. FLYCHK[3], an atomic non-LTE code designed to provide ionization and population distributions, will be used to diagnose the plasma temperature, density and ionization states. This information will ultimately be used to gain insight into how the plasma conditions affect the production of positrons. Comparisons will also be made between Au and Eu plasmas for similar laser conditions.

References

[1] Kneip, S. *et al.* HEDP **4** 41-48 (2008)
[2] Jiang, Z. *et al.* Phys. Plasmas **2** 5 1702-1711 (1995)
[3] Chung, H. *et al*. http://nlte.nist.gov/FLY/ (2008)

Betatron X-Ray Spectra from a Laser Wakefield Accelerator Using Ionization Injection

Will Schumaker [a], C. McGuffey [a], A.G.R. Thomas [a], A. Maksimchuk [a], G. Kalintchenko [a], V. Chvykov [a], V. Yanovsky [a], K. Krushelnick [a], S. Kneip [b], M. Bloom [b], S. Mangles [b], Z. Najmudin [b]

(a) University of Michigan, Ann Arbor, MI 48109 (wschumak@umich.edu)
(b) Imperial College London

Electron beams typically produced by the HERCULES laser wakefield accelerator can be characterized as being of relatively high charge (~100 pC) in femtosecond duration, quasi-monoenergetic bunches. Oscillations of these electrons in the electromagnetic
fields of the plasma bubble cavity created by laser driven ponderomotive expulsion can lead to extremely bright sources of X-rays in the 5-100 keV energy range. Such configurations are proposed as future sources of radiation for a number of applications, as their compact size and potential low cost is highly attractive, and may enable such facilities to be more widely available to the scientific, medical and engineering communities. To help understand and explore this phenomena, experimental measurements of X-ray spectra from laser wakefield accelerated electrons that are ionization-injected will be presented in comparison to X-ray spectra resulting from self-injection across various plasma densities and laser powers.

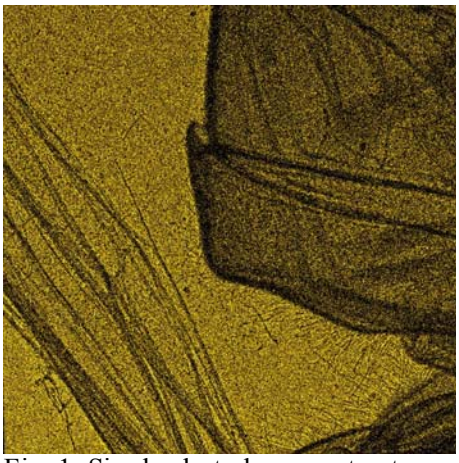

Fig. 1: Single-shot phase-contrast radiograph of a Yellow Jacket's abdomen and antennae using the HERCULES laser. Fine hair structure along the abdomen correlates with our source size of <10µm.

References

[1] S.P.D. Mangles et al., Nature **431**, 535 (2004)
[2] C.G.R. Geddes et al., Nature **431**, 538 (2004)
[3] J. Faure et al., Nature **431**, 541 (2004)
[4] C. McGuffey et al., Phys. Rev. Lett. **104**, 025004 (2010)
[5] S. Kneip et al., Phys. Rev. Lett. **100**, 105006 (2008)

Multi-Layered Richtmyer-Meshkov Instability

Pooya Movahed, Eric Johnsen

Department of Mechanical Engineering, University of Michigan, Ann Arbor (pooyam@umich.edu)

Inertial Confinement Fusion (ICF) is a promising source of energy and the National Ignition Facility (NIF) is making significant steps toward making fusion energy accessible. Hydrodynamic instabilities such as the Richtmyer-Meshkov (RM) instability occur during the ICF process reduce the efficiency of the burning process.[1] Hence, a better understanding of the RM instability is required.

The RM instability occurs when a shock interacts with a perturbed interface separating fluids of different densities. Analytical results can be obtained for small-amplitude linear growth of a single mode. Experimental results show good agreement with the theory at early times but as the amplitude of the perturbation increases or when the geometry or problem set-up is more complex, the linearized equations do not apply anymore.

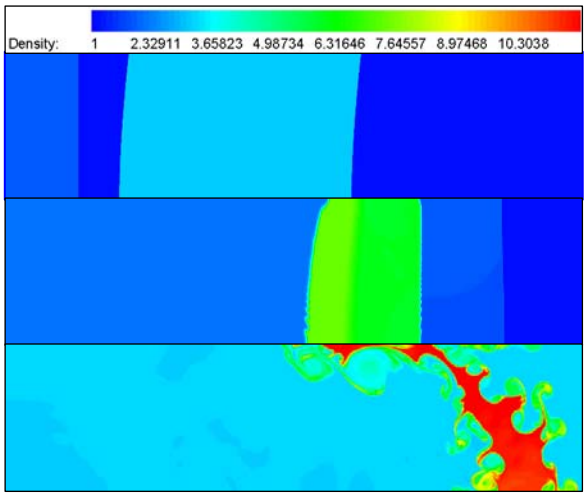

Fig. 1: Density countours of air/SF6/air gas combination for multi-layered Richtmyer-Meshkov instability at three different time stages.

In this paper, a numerical study has been carried out to gain a better understanding of the multi-layered RM instability. A parallel second order accurate MUSCL-Hancock scheme is used to solve the Euler equations with a γ-based model for the multi-fluid equations. In this approach, the advection equation for γ is solved in a non-conservative form to prevent pressure oscillations at the interface.[2] Using the same definition as in the experiments, we identify the location of the interface and a comparison of the bubble speed velocity with experiments is used to validate our numerical results.[3]

Fluids such as air, SF6 and R22 with different Atwood numbers and configurations are used to investigate the mixing phenomena occurring at the interface. In Fig. 1(top), density contours of the initial configuration of air/SF6/air gas combination with M=1.5 are shown. Non-reflecting boundary conditions are specified along the left boundary, and the remaining boundaries are solid walls. The baroclinc vorticity generation along the interface due to the passage of the initially right moving shock is the main mechanism for the amplitude amplification at the first interface (positive Atwood number) and the phase change at the second interface (negative Atwood number). In Fig. 1(middle), the shock has passed interfaces and a rarefaction wave is moving toward the first interface. The perturbation amplitude is still small before the reshock. After the reshock (Fig. 1(bottom)), the flow becomes completely nonlinear and the Kelvin-Helmholtz shearing instability also occurs which leads to mushroom like structures and some mixing regions.

References

[1] S. Taylor and P. Pix, Commun. Pure Appl. Math. **13**, 297 (1960).
[2] R. Saurel and R. Abgrall, SIAM J. Sci. Comput. **21**, 1115 (1999).
[3] O. Sadot et al., Phys. Rev. Lett. **80**, 1654 (1998).

A High-Repetition Rate LWFA for Studies of Laser Propagation and Electron Generation

Zhaohan He, James Easter, Bixue Hou, Karl Krushelnick, John Nees and Alec Thomas

Center for Ultrafast Optical Science, University of Michigan, Ann Arbor

Advances in ultrafast optics today have enabled laser systems to deliver ever shorter and more intense pulses. When focused, such laser pulses can easily exceed relativistic intensities where the wakefield created by the strong laser electric field can be used to accelerate electrons. Laser wakefield acceleration of electrons holds promise for future compact electron accelerators or drivers of other radiation sources in many scientific, medical and engineering applications. We present experimental studies of laser wakefield acceleration using the λ-cubed laser at the University of Michigan -- a table-top high-power laser system operating at 500 Hz repetition rate. The high repetition rate allows statistical studies of laser propagation and electron acceleration which are not accessible with typical sub-0.1 Hz repetition rate systems. In addition, we compare the experiments with particle-in-cell simulations using the code OSIRIS.

Narrow Energy Spread Proton and Ion Spectra from High-Intensity Laser Interactions

Franklin Dollar [a], Takeshi Matsuoka [a], Chris McGuffey [a], Stepan S. Bulanov [a], Vladimir Chvykov [a], Jack Davis[b], Galina Kalintchenko [a], George Petrov[b], Alec G. R. Thomas [a], Louise Willingale [a], Victor Yanovsky [a], Anatoly Maksimchuk [a], and Karl Krushelnick [a]

(a) Center for Ultrafast Optical Science, Univ. Of Michigan, Ann Arbor (fjdollar@umich.edu)
(b) Naval Research Laboratories, Washington, DC

Recent simulations show that an idealized, high intensity, short pulse laser can generate quasi-monoenergetic proton beams with energies over 100 MeV in an interaction with a thin film[1]. However, most short pulse laser facilities with sufficient intensity lack the nanosecond and picosecond constrast necessary to realize such a regime. Experiments were performed to investigate proton and ion acceleration from a high contrast, short pulse laser by employing dual plasma mirrors along with a deformable mirror at the HERCULES laser facility at the Center for Ultrafast Optical Sciences, University of Michigan. Plasma mirrors were characterized, allowing a 50% throughput with a contrast increase of 10^5. The focal quality was also characterized, showing a 1.1 micron full width at half maximum (FWHM) focal diameter. Experiments were done using temporally cleaned 30 TW, 32fs pulses to achieve an intensity of up to 10^21 W/cm2 on Si3N4 and Mylar targets with thicknesses ranging 50nm to 13 um. Proton beams with energy spreads below 75% were observed from all thicknesses, peaking with energies up to 10.3 MeV and an energy spread of 25% FWHM [fig 1]. Similar narrow energy spreads were observed for oxygen, nitrogen, and carbon at the silicon nitride thickness of 50nm with energies up to 2 MeV per nucleon with an energy spread of 23%, whereas the energy spread is greatly increased at higher thicknesses. Maximum energies were confirmed with CR39 track detectors, while a Thomson ion spectrometer was used to gauge the monoenergetic nature of the beam. 2D PIC simulations were also performed at parameters representative of the experimental conditions.

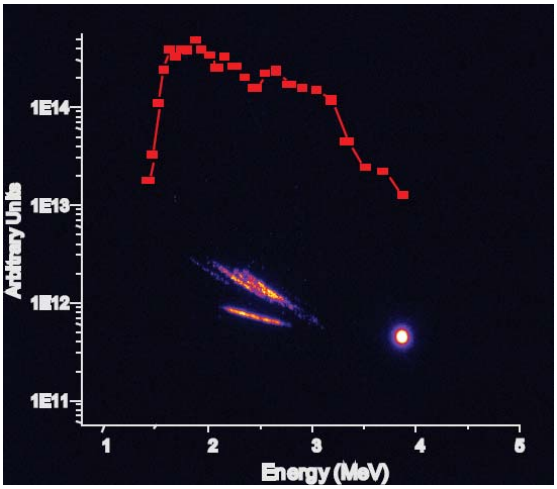

Fig. 1: Raw ion spectrometer trace and the corresponding proton energy spectra for 50nm Si3N4 membranes with prepulse present.

References

[1] S. S. Bulanov, et al., "Acceleration of monoenergetic protons from ultra-thin foils by flat-front laser pulses in the Directed Coulomb explosion regime" Phys. Rev. E 78, 026412 (2008).

A Computational Investigation of the Impact of Non-Gaussian, "Low-Quality" Laser Pulses on Electron Beam Properties in Laser-Wakefield Acceleration Experiments

P. G. Cummings and A. G. R. Thomas
Center for Ultrafast Optical Science, The University of Michigan
(cummingp@umich.edu, agrt@umich.edu)

The impact of non-Gaussian, "low-quality," laser pulse profiles on the performance of laser- wakefield acceleration (LWFA) experiments is investigated computationally using the particle-in-cell simulation code OSIRIS 2.0. A baseline simulation of a TEM00-mode (Gaussian) pulse is performed, and the properties of the electron beam produced by this pulse are measured.

This pulse is then "mixed" with a TEM10-mode pulse across a range of mixing percentages (while maintaining a constant total pulse energy), as a preliminary investigation into the effects of non-Gaussian pulse profiles on LWFA performance. Scalings relating the divergence, emittance, and peak pulse energy of the LWFA-produced electron beam to the mode mixing percentage are established.

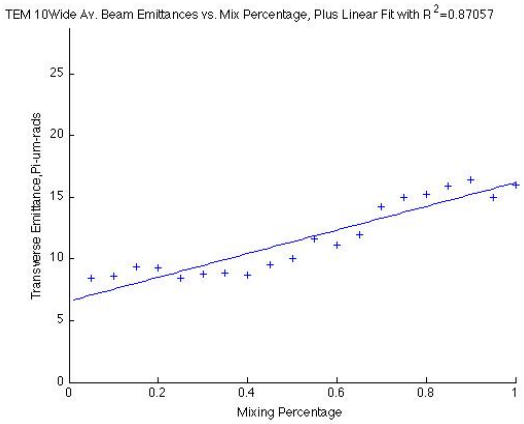

Fig 1: The transverse emittance of the final electron beam vs. mixing percentage for the simple TEM-mode-mixing simulation sweep

Using this simplified parameter sweep as a reference, more complex simulations of LWFA experiments with optical aberrations including comaticities, astigmatisms, and spherical aberrations are performed and analyzed. Modifications to OSIRIS to enable the explicit inclusion of these aberrations are discussed.

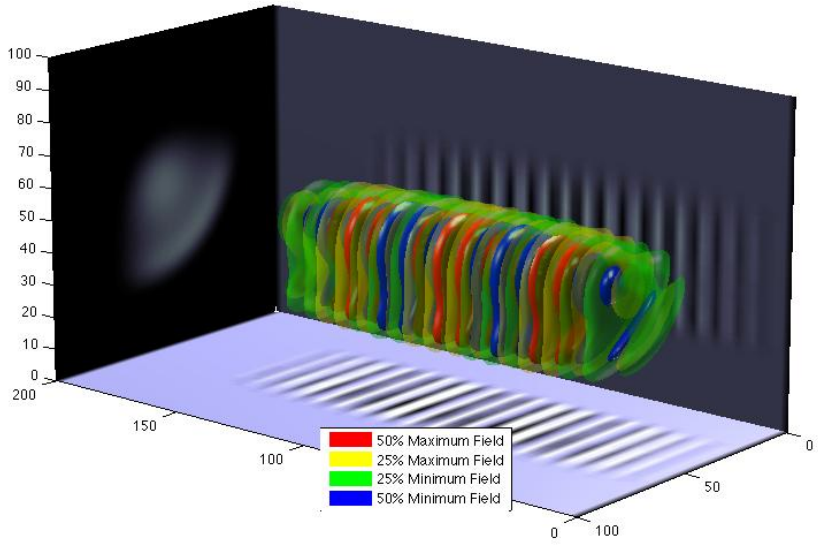

Fig 2: The initialized pulse from OSIRIS, modified to include a comatic aberration with a Strehl ratio of 0.417.

Radiative Stabilization of Rayleigh-Taylor Instabilities in Supernova-Relevant Experiments on the National Ignition Facility

Channing M. Huntington [a], Carolyn C. Kuranz [a], R. Paul Drake [a], Aaron R. Miles [b], Hye-Sook Park [b], Shon T. Prisbrey [b], Bruce A. Remington [b]

(a) Atmospheric Oceanic, Space Science, University of Michigan, Ann Arbor, MI 48103 (channing@umich.edu)
(b) Lawrence Livermore National Laboratory, Livermore, CA 94550

We are performing an experiment on the National Ignition Facility (NIF) to investigate supernovae-relevant Rayleigh-Taylor instability growth in a planar geometry. This experiment uses a NIF indirect drive platform to launch a strong shock (>100 Mbar initial pressure) into a foam and iodinated plastic target. A rippled perturbation machined into the plastic-foam interface seeds the Rayleigh-Taylor (RT) instability, which quickly transitions into the non-linear regime during the experiment. Unlike similar previous experiments [1], the shock produced by the NIF drive is strongly radiative in the low-density foam, and this radiation will modify the structure and dynamics of the system [2]. In this radiative regime the instability growth is expected to be lower than that in a non-radiative shock, and the traditional RT growth rates must be modified.

Fig. 1: Experimental target fielded on the NIF. A gold hohlraum is mounted on a positioning stalk and used to create the x-ray drive. An aluminium sphere protects the experimental package from unconverted laser light.

To elucidate the dynamics of the system, simulations were performed using the radiation hydrodynamics code HYDRA [3]. Simulation results allowed calculation of modified analytic RT growth rates which have been proposed in the literature. These calculations show a reduced RT spike growth as a result of the decrease in density gradient in strongly driven targets. This result is quantified over a range of drive temperatures and compared between several target materials and densities. Additionally, the effect of non-thermal gold M-band x-rays which serve to preheat the unstable interface is investigated. This work has direct applicability to the observable features in the upcoming NIF experiment.

References

[1] C.C. Kuranz et. al. *Astrophys. J.* **696** 749-759 (2009)
[2] C.C. Kuranz et. al. *Astrophysics and Space Science,* Submitted.
[3] M. M. Marinak et al. Phys. Plasmas **8** 2275 (2001)

This work was performed under the auspices of the Lawrence Livermore National Security, LLC, (LLNS) under Contract No. DE-AC52-07NA27344 and by the NNSA-DS and SC-OFES Joint Program in High-Energy-Density Laboratory Plasmas, grant number DE-FG52-09NA29548.

Guided Corona Generates Wettability Patterns That Selectively Direct Cell Attachment Inside Closed Microchannels

Angela Dixon [a] and Shuichi Takayama [a, b]

(a) Department of Biomedical Engineering, University of Michigan
(b) Department of Macromolecular Science and Engineering
(takayama@umich.edu)

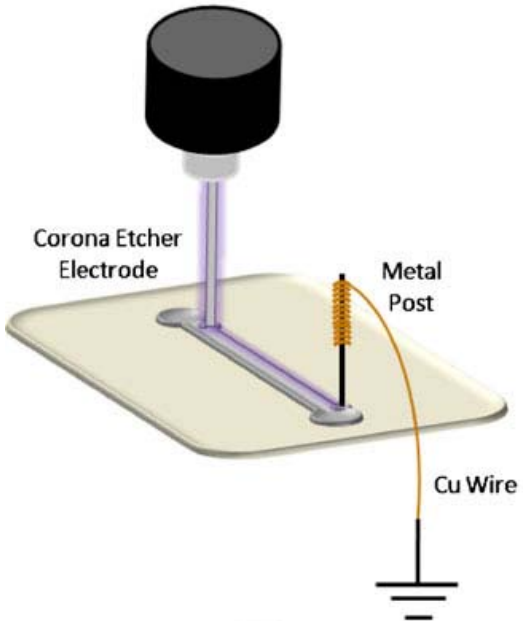

Fig. 1 Set-up for Biased In-Channel Corona Etching includes the integration of a corona treater, metal post and copper wire.

We present a method to create plasma mediated linear protein patterns along the lengths of simple one-inlet-one-outlet straight polydimethylsiloxane microchannels by biasing the delivery of corona discharge at the capillary openings. Pattern widths ranging from 500–1,000 μm were generated in 2 mm wide microchannels with lengths of 0.5, 1.0, or 1.5 cm. Corona-treated surfaces enabled the spatial alignment of C2C12 myoblasts to the adhesive protein-coated regions, facilitating myoblast differentiation into myotubes. Although limited in preci sion, this protein patterning technique offers the advantages of simplicity and low cost, making it attractive for educational and research environments that lack access to extensive microfabrication facilities. The results also provide a cautionary note to those using corona discharge to increase wettability of microchannels; the surface modification may not be uniform, even within single microchannels being treated depending on settings and positioning of the corona device tips.

Recirculating Planar Magnetrons: Simulations and Experiment

Matthew Franzi [a], Ronald Gilgenbach[a] , YY Lau [a] , David French [a]

Brad Hoff [b], David Simon[a]

(a) Plasma, Pulsed Power and Microwave Lab, Nuclear Engineering and Radiological Sciences Dept., University of Michigan, Ann Arbor, MI 48109-2104 (mfronz@umich.edu)

(b) Air Force Research Lab, Kirtland AFB, NM

The Recirculating Planar Magnetron (RPM) is a novel cross-field device whose unique geometry is expected to provide numerous operational advantages over current HPM devices. The preliminary configuration of this magnetron consists of two parallel planar sections which joined on either end by cut cylindrical regions to form a concentric extruded ellipse. The device is aptly named the RPM for its inherent ability to maintain or re-circulate the electron beam from one planar regime to the other. The circulating electron beam will interact with several resonant cavities placed on the anode causing synchronous electron bunching. Resultant groups of space charge will then readily drive a RF electric field in the cavities which may be extracted to waveguides. The RPM may be designed in either a conventional configuration with the anode on the outside, for simplified extraction, or as an inverted magnetron with the anode as in the inner conductor which reduces the start-up time of the device. The advantages of either configuration include higher current yield and faster heat dissipation due to the larger surface area.

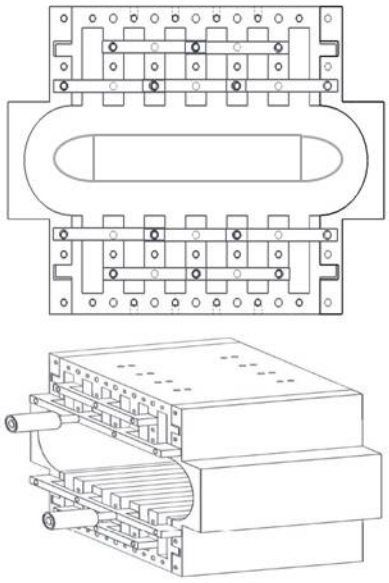

Figure1: Line sketch of conventional RPM: front (top) Oblique (bottom)

Currently, experiments at the Pulsed Power and Microwave Laboratory at the University of Michigan are in the setup and design phase. A conventional RPM with planar cavities is to be installed on the Michigan Electron Long Beam Accelerator (MELBA) and is anticipated to operate at ~250kV, 0.2T with a beam current of 1-10kA at 1GHz. Simulations have shown HPM pulses in the realm of 100s of MW with pulse lengths on the order of 1μs due to plasma closure of the AK gap. Future work will include the design and analysis of an inverted configuration as well as an investigation of several mode priming techniques previously conducted at the University of Michigan.

Electron Dynamics in Crossed Field Devices

David M. French [a], David H. Simon [a], Y.Y. Lau [a],
Ronald M. Gilgenbach [a], Brad Hoff [b], John Luginsland [c]

(a) University of Michigan, Ann Arbor, MI
(dmfrench@umich.edu, dhsimon@umich.edu, yylau@umich.edu, rongilg@umich.edu)
(b) Air Force Research Laboratory, Kirtland AFB, NM (brad.hoff@kirtland.af.mil)
(c) Air Force Office of Scientific Research, Arlington, VA (john.luginsland@afosr.af.mil)

Recently there has been a renewed interest in the inverted magnetron because of its larger cathode area, reduction of electron end-loss, and substantially faster startup in comparison with the conventional magnetron. A recently conceived embodiment of the magnetron, called the recirculating planar magnetron, RPM [1], incorporates these attractive features. The electron dynamics for the various magnetron configurations has been re-examined with the Particle-In-Cell code MAGIC.

It has been shown [2] that an electron rotating under a combination of axial magnetic field B_0 and a radial electric field E_0 has an effective mass in the *azimuthal* direction, which can be either positive or negative depending on the magnitude and sign of E_0. For inverted magnetron, this effective mass is negative, therefore an azimuthal electron density bunching (a spoke) has a tendency to build up. For conventional magnetrons, this effective mass is positive, and the tendency toward azimuthal bunching disappears, at least during startup.

We believe that this negative-mass property in the inverted magnetron leads to its substantially faster startup than the conventional magnetron. The results of simulations showing the initiation of bunching in several different magnetron configurations, including the RPM will be presented.

Research supported by AFOSR, AFRL, L-3 Communications Electron Device Division and Northrop-Grumman Corporation.

References

[1] R. M. Gilgenbach et al., "Recirculating-Planar-Magnetron for High Power, High-frequency Raddiation Generation," ICOPS Conference 2010.

[2] D. Chernin and Y. Y. Lau, Phys. Fluids 27, 2319 (1984); Y. Y. Lau, Phys. Rev. Lett. 53, 395 (1984); and in Ch. 9 in High Power Microwave Sources, Eds. V. L. Granatstein and I. Alexeff (Artech House, 1987).

Cathode Spot Ejected Particle Image Velocimetry (PIV) Calculations

Eric D. Gillman [a], John E. Foster [a] and Isaiah M. Blankson [b]

(a) University of Michigan, Dept. of Nuclear Engin. and Radiological Sci.
(edgill@umich.edu, jefoster@umich.edu)
(b) NASA Glenn Research Center (Isaiah.m.blankson@nasa.gov)

Spacecraft reentering the atmosphere at hypersonic velocities and other hypersonic vehicles are enveloped by a layer of plasma, commonly referred to as the 'plasma sheath'. This plasma envelope is caused by a hypersonic shock and frictional heating of air as it passes around the hypersonic vehicle. The layer of plasma blocks and prevents transmission and reception of communication signals below the plasma cutoff frequency.

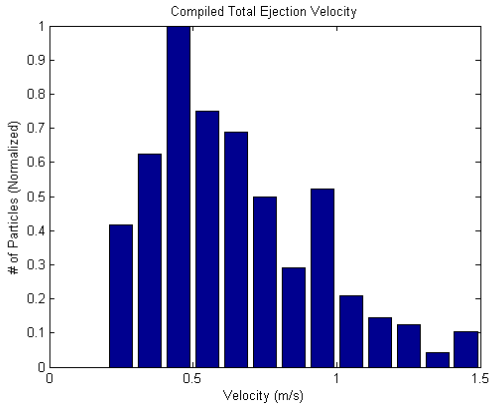

Fig. 1: Distribution of ejection velocity of dust particles as they are ejected from the electrode surface by cathode spots.

A method of plasma 'quenching' via fine particulate dispersal is being investigated to reduce the plasma cutoff frequency. Cathode spot plasma plumes are utilized to disperse ceramic powder into an overhead radio frequency (RF) plasma used to simulate the reentry plasma. As the ceramic particles are ejected and travel through the plasma, the particles will collect electrons as they float to the plasma floating potential, reducing the electron density.

The velocity at which these particles are ejected is of significant importance for practical implementation of this mitigation method. Particle imaging velocimetry methods are used to obtain particle velocities. Using basic conservation of energy equations, we are able to determine the velocity of particles at the time of their ejection from the electrode surface. The distribution of the ejection velocity is shown in figure 1. Further analysis reveals interesting trends in the components of velocity transferred to the particles via cathode spots. In addition, a particle witness plate and captured images provide further information on the mechanisms involved with cathode spot dispersion of ceramic powder.

References

[1] Jones, C.H., AFOSR Workshop on Communications Through Plasma During Hypersonic Flight, Aug. 2006.
[2] Ryback, J.P., and R.J. Churchill, IEEE Trans. On Antennas and Propagation, Vol. AES-7, No. 5, Sept. 197 1, pp. 879-894.
[3] Chen, F.F., Introduction to Plasma Physics and Controlled Fusion, Plenum Press, New York (1984).
[4] Boxman, R., et. al, Handbook of Vacuum Arc Science and Technology, Park Ridge, NJ: Noyes, 1995

Investigation of Plasma Formation and Evolution in Post-Hole Convolutes

M. R. Gomez [a], R. M. Gilgenbach [a], M. E. Cuneo [b],
R. D. McBride [b], J. E. Bailey [b], G. A. Rochau [b], and P. W. Lake [b]

(a) Plasma, Pulsed Power, and Microwave Lab, Nuclear Engineering and Radiological Sciences Department, University of Michigan – Ann Arbor, MI 48109
(mrgomez@umich.edu)

(b) Sandia National Labs, New Mexico, P.O. Box 5800, Albuquerque, NM 87185

A post-hole convolute is a geometric arrangement in which two electrodes of the same polarity are connected to one another via a conductor through a hole in an intermediate electrode with the opposite polarity. Post-hole convolutes are a necessary component of Load Current Multipliers and can also be used to combine current from several self-magnetically insulated transmission lines. Post-hole convolutes have become an important component of many large pulsed power devices, but there has not been a detailed experimental study of post-hole convolute performance.

A recent upgrade to the Z Machine at Sandia National Labs increased the maximum current that the driver could supply, but also significantly increased current losses in the post-hole convolute (losses on the order of 20% have been observed). The purpose of this research is to determine the relevant parameters of the plasma formed in a post-hole convolute (plasma composition, plasma source, electron temperature, plasma density, turn-on time, closure velocity, etc.) and their effect on convolute performance. Experimental studies are currently underway on the Z Machine at Sandia National Labs.

Spatially Resolved Study of Inter-Cusp Transport and Containment of Primary Electrons

Aimee A. Hubble [a], John E. Foster [b]

(a) University of Michigan, Department of Nuclear Engineering and Radiological Sciences (aahubble@umich.edu)

(b) University of Michigan, Department of Nuclear Engineering and Radiological Sciences (jefoster@umich.edu)

Electron current density profiles were obtained in the region above two magnetic cusps in a 20 cm partial conic ring cusp ion thruster discharge chamber. The density profiles were obtained by use of a translatable Langmuir probe and an automated motion stage and data collection system. These high-resolution density profiles allowed for the study of electron collection mechanics in the absence of gas flow and plasma production, as well as at varying levels of gas flow. An internal pressure sensor mounted in the discharge chamber allows for accurate measurements of chamber collisions. This is the second stage in a series of experiments aimed at better understanding collection physics at the magnetic cusps during discharge chamber operation. The current density maps allow for particle transport through the cusps to be visualized, and see how discharge chamber geometry plays a role in collection. Attenuation coefficients and loss widths as a function of probe distance above the anode were calculated from the current density data, and compared at a variety of discharge currents. In addition, these current density maps were compared to those obtained using a planar and line cusp source geometry, to study how source geometry affects particle collection. Results will be compared to a line-cusp source to evaluate the effect of cusp symmetry on collection.

Time-Resolved Electron Energy Distribution Functions: Preliminary Results and Development of a Rapidly Swept Langmuir Probe System

Robert B. Lobbia and Alec D. Gallimore

The University of Michigan, Ann Arbor
(lobbia@umich.edu, alec.gallimore@umich.edu)

Measurement of the constantly shifting state of energy equilibrium in a transient plasma discharge is vital in enhancing undersanding that may be applied to achieve improved device performance through the minimizing of identified transient loss processes. To perform these measurements, a unique rapidly swept Langmuir probe system is presently under development that enables the acquisition of various plasma properties including the electron and ion densities, the plasma and floating potentials, and the electron temperature and electron energy distribution function (EEDF)—all simultaneously at a continuous rate of 1 μs (for seemless sets in excess of 5 s). This direct approach of rapidly sweeping a Langmuir probe is challenged by the hardware requirements that include broadband (DC-100 MHz), high-voltage (±200 V), large dynamic range (nA to 100 mA), and low signal-to-noise (80 dB) sensors coupled to fast (180 MHz) 16-bit digitizers interfaced (at >3GB/s) to deep memory reserves (48 GB). The transient properties of a turbulent plasma discharge, accurately captured with this system, along with turbulent statistical correlations computed from these data will provide insight into the dynamics of various unsteady plasma devices (e.g. pulsed plasmas, Hall thrusters, RF discharges, etc.). This new high-speed electrostatic plasma diagnostic builds upon the success of an earlier developed high-speed Langmuir probe system (combined with a novel noise and capacitance compensation electrode) with a 10 μs temporal resolution.[1] One of the dramatic features of a rapidly swept Langmuir system with low-noise sensors, is the unfiltered smoothness of the collected current-voltage (*I-V*) probe data, thus enabling direct numerically computed second derivatives that do not require any smoothing. In this manner, time-resolved EEDFs are computed according to the Druyvesteyn method, thereby providing a measurement of the transient state of energy balance within the plasma. Preliminary time-resolved EEDFs and other plasma properties are presented for sweep rates 100 kHz - 1 MHz within the downstream plume of a Hall thruster where the expected maximum sweep rate is 1-10 MHz.[2] These data demonstrate that the discharge from a Hall thruster is rich in dynamic character, and that identified transient (thruster breathing mode coupled) non-Maxwellian high-energy electrons may be responsible for the enhanced ionization efficiency of these devices.

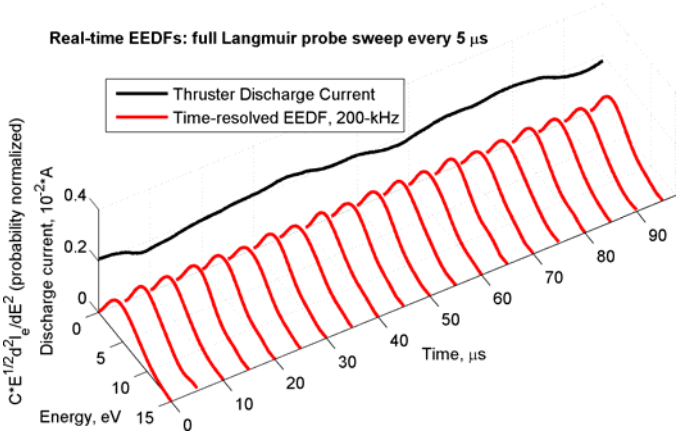

Fig. 1: Rapidly acquired preliminary EEDF data 1.5 m downstream from a 6 kW Hall effect thruster (xenon plasma) with simultaneously measured dischage current.

References

[1] R. Lobbia and A. Gallimore, Rev. Sci. Instrum., 073503, Vol. 81, Issue 7, July 2010.
[2] R. Lobbia and A. Gallimore, Physics of Plasmas, 073502, Vol. 17, Issue 7, July 2010.

Modeling Reaction Rates in Ar/N_2 ICP Plasmas Using Pulsed Power for a Variety of Duty Cycles, Pressures, Average Powers, and Frequencies*

Michael D. Logue and Mark J. Kushner
Department of Electrical and Computer Engineering
University of Michigan, Ann Arbor, MI 48105 USA
(mdlogue@umich.edu, mjkush@umich.edu)

Of great interest to the development of plasma processing is the ability to better control the electron energy distribution, $f(\varepsilon)$, which can allow for better selectivity of reactants produced by electron impact excitation and dissociation. This is particularly important in low pressure, inductively coupled plasmas (ICPs) where dissociation products often react with surfaces before other gas phase species, and so these fluxes are most directly a function of electron impact rate coefficients. The control of $f(\varepsilon)$, and so the reaction rate coefficients, can be achieved by varying the pressure, and power, as well as using pulses of power. It is the latter case which we will focus on.

In this paper, we discuss results from a computational investigation of reaction rate coefficients in Ar/N_2 gas mixtures at pressures of tens of mTorr in ICPs. The investigation was conducted with the Hybrid Plasma Equipment Model (HPEM) with which $f(\varepsilon)$ as a function of position and time are obtained using a Monte Carlo simulation. The rf frequency is 5-50 MHz (base case 20 MHz) with the pulse power having a PRF (pulse repetition frequency) of 100-800 KHz (base case 100 KHz). Time dependent and PRF averaged $f(\varepsilon)$ will be discussed as a function of duty cycle, pressure, PRF averaged power and frequency, and rf frequency. To monitor the effects of these quantities on rate coefficients, k, the excitation of $N_2(v=1)$ and $N_2(A)$, as well as the ionization of Ar will be monitored as representing low, intermediate and high threshold processes. In particular we will focus on the n_e*k product as a representative of the source function for the three processes, which should provide a better idea of the generation rate of that particular species.

We found that the modification of $f(\varepsilon)$ seemed to be mostly localized to near the coils. We also found that there was much greater variation of the n_e*k product during the pulse for the higher threshold processes. We found that the n_e*k product seems to increase with increasing PRF averaged power and/or decreasing duty cycle. Strategies will be discussed to optimize the shape of $f(\varepsilon)$ to emphasize a particular process.

*Work supported by the Department of Energy Office of Fusion Energy Science.

Fluorocarbon Polymer Removal in H_2/He Plasmas with NH_3 Plasma Sealing of Porous Low-*k* Dielectric*

Juline Shoeb [a] and Mark J Kushner [b]

(a) Iowa State Univ., Dept. Electrical & Computer Engineering (jshoeb@eecs.umich.edu)
(b) Mark J. Kushner, Univ. of Michigan, Elect. Engr. & Comp. Sci. (mjkush@umich.edu)

Porous dielectric materials are being used to lower the interconnect capacitance to limit the RC time delay in integrated circuits. SiCOH, silicon dioxide with CH_x groups lining the pores, is one commonly used porous material. Fluorocarbon plasmas are used to etch a porous SiCOH while organic photoresist (PR) materials are used to define the feature. Both the PR and fluorocarbon polymers left in the feature must be removed. If an oxygen containing plasma is used to remove the polymer and PR, reactive oxygen species can remove CH_3 groups from the SiCOH, thereby increasing the dielectric constant. Consequently, H_2/He plasmas have been investigated to remove the polymer and PR. The light mass of H atoms and endothermic nature of many of such reactions require hot H atoms for these removal processes. Franck-Condon heating and relaxation of vibrational states of hydrogen molecules can generate H atoms with energy as high as 10 eV, while charge exchange reactions can produce H atoms with tens of electron volts. To maintain the low *k* values of porous dielectrics, sealing of the surface pores is desirable. H_2/He treatment can remove H atoms from Si-CH_3 creating reactive sites, and successive NH_3 plasmas can seal pores creating Si-N and C-N bonds while maintaining the low-*k* value of the porous dielectric.[1]

In this talk, we discuss results from a modeling of the PR removal, polymer cleaning and sealing of a porous carbon doped silica film (SiOCH). A reaction mechanism was developed for plasmas sustained in H_2/He and NH_3/Ar mixtures and their interactions with the low-*k* porous material. The Hybrid Plasma Equipment Module was employed to obtain the energy and angle distributions for species incident on the surface in H_2/He and NH_3/Ar mixtures. The cleaning and sealing reaction mechanism was implemented into Monte Carlo Feature Profile Module with which profiles of the low-*k* material after the plasma exposures are predicted. Results will be discussed, including validation with data from the literature, for the densification and sealing of pores as a function of treatment time, bias and plasma power.

References

[1] A. M. Urbanowicz, et al. Electrochem. Solid-State Lett. **10**, G76 (2007).

* Work supported by the Semiconductor Research Corp.

Control of Electron Energy Distributions and Flux Ratio in Pulsed Capacitively Coupled Plasmas with Different Duty Cycle and Pulse Repetition Frequency*

Sang-Heon Song [a] and Mark J. Kushner [b]

(a) Nuclear Engineering and Radiological Sciences (ssongs@umich.edu)
(b) Electrical Engineering and Computer Science (mjkush@umich.edu)
University of Michigan, Ann Arbor, MI 48109 USA

In capacitively coupled radio frequency (rf) discharges, as used in plasma processing of semiconductor materials, controlling the electron energy distribution function $f(\varepsilon)$ is important for controlling the flux of radicals and ions to the substrate. The strategies for controlling $f(\varepsilon)$ include varying duty cycle and pulse repetition frequency in different gas mixtures. Customizing the $f(\varepsilon)$ is related to balancing the electron heating and cooling mechanisms. Multi-frequency capacitively coupled plasmas (CCPs) provide an opportunity to customize $f(\varepsilon)$ through using pulsed plasmas. For example, a low frequency (LF) is typically applied to the lower electrode to control ion energy distributions and a high frequency (HF) is applied to the upper electrode to heat electrons. By pulsing the HF one can modulate $f(\varepsilon)$ to produce shapes that are not otherwise attainable using continuous wave excitation. For example, an $f(\varepsilon)$ may be produced that has both a high energy tail and a large thermal component. These $f(\varepsilon)$ will produce different dissociation patterns in the feedstock gases. Also the feedstock gases produce different $f(\varepsilon)$ due to different heating and cooling mechanism. The choice of duty cycle and pulse repetition frequency (PRF) are important to the time average $f(\varepsilon)$ as these determine the relative role of thermalization.

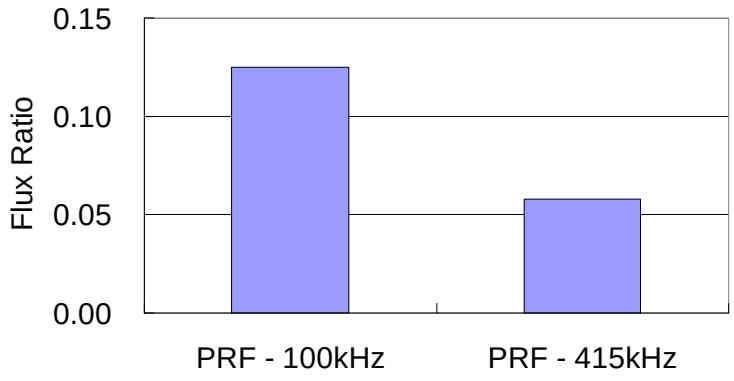

Fig. 1: The flux ratio of argon excited species to total ion flux onto the substrate. The reduced pulse repetition frequency makes a larger flux ratio of argon excited species.

The customization of $f(\varepsilon)$ in 2-frequency CCPs will be discussed using results from a 2-dimensional plasma equipment model. The electron $f(\varepsilon)$ are obtained using a Monte Carlo simulation including electron-electron collisions. The consequences of PRF, duty cycle and HF power on $f(\varepsilon)$ will be discussed for pressures of tens of mTorr in argon and fluorocarbon gas mixtures. The correlation between these parameters and $f(\varepsilon)$ on the identity of radical and ion fluxes onto the substrate will be made. One of the results is shown in Fig. 1 that represents the manipulated flux ratio by PRF.

* Work supported by the Department of Energy Office of Fusion Energy Sciences and the Semiconductor Research Corp.

Fabrication of 3D Carbon Nanotube Microstructures by Capillary Forming

Sameh Tawfick [a], Michael De Volder [a,b] , Sei Jin Park [a], Davor Copic [a], and A. John Hart [a]

(a) Mechanosynthesis Group, University of Michigan (ajohnh@umich.edu)
(b) IMEC, Belgium

We present a method for high-throughput fabrication of robust three-dimensional (3D) carbon nanotube (CNT) microforms, which creates delicate and heterogeneous geometries in close proximity and over large areas [1]. This method, called capillary forming, is based on our finding that condensation of liquid onto vertically aligned CNT microstructures, followed by evaporation, causes a deterministic transformation of the individual structures to intricate 3D shapes. We have fabricated a diverse set of forms having controllable bends, twists, and re-entrant curves, and patterns having complex arrangements of in-plane and out-of-plane features. These include arrays of CNT pins, needles, and cones made of closely-packed aligned CNTs, which may be useful as field emitters. Owing to the mechanical robustness and anisotropic electrical conductivity of CNTs, we also demonstrate applications of these novel CNT structures as master molds for mass-production of 3D polymer structures and responsive hydrogel microactuators.

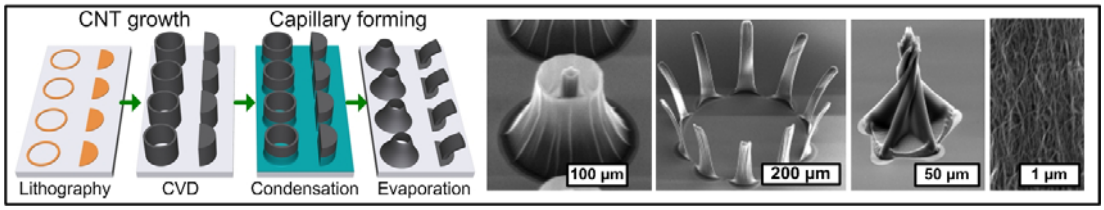

References

[1] M. Devolder, S. Tawfick, et al., Advanced Materials, in press 2010.

Different Patterns of High-Energy and Low-Energy Electrons in an Atmospheric-Pressure Microplasma Generated by a Hairpin Resonator

Wei Tian [a,b], Xi-Ming Zhu [a] and Yi-Kang Pu [a]

(a) Tsinghua University, Department of Engineering Physics, Beijing 100084, People's Republic of China
(b) University of Michigan, Department of Nuclear Engineering and Radiological Science, Ann Arbor, MI 48109, (bucktian@umich.edu.cn)

A new device, hairpin resonator, is used to generate an atmospheric-pressure argon microplasma with a microwave power supply. The hairpin resonator consists of a U-shaped copper line, on which the microwave resonates, and a coupling loop, which transmits power into the U-shaped line (Figure (a)). The hairpin resonator discharge consists of three discharge balls (Figure (b)). A spatially resolved optical system is used to obtain the two-dimensional distributions of the intensity of argon emission lines in the microplasma. For the first time, it is found that the high- and low-energy electrons (with energy ~ 10 eV and ~ 1 eV) in the microplasma have different spatial patterns (Figure (c)). Most of the high-energy electrons are in the center of each discharge ball, while the low-energy electrons remain uniform in and around the discharge balls. An argon collisional-radiative model is built to relate the electron densities to the emission spectra. From this model, the density distribution of high-energy electrons is obtained from the emission line intensity, while the density distribution of low-energy electrons is deduced from the intensity ratios of several different emission lines. The difference in the spatial distribution between the two groups of electrons is mainly due to the different energy-loss characteristic lengths of them in the atmospheric-pressure microplasma.

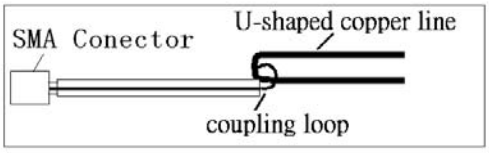

(a) The structure of the hairpin resonator is shown.

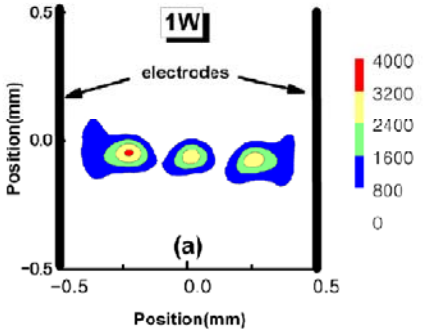

(b) It shows the contour of emission line intensities at 1 W and the electrodes kept at 1 cm.

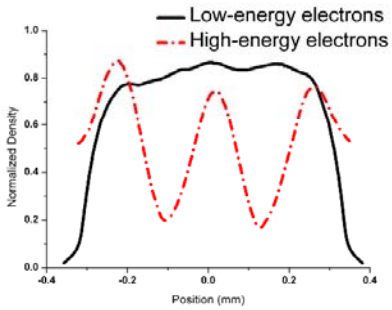

(c) The solid line presents the high-energy electrons; the dashed line presents the low-energy electrons.

Electron Current Extraction from RF Excited Micro-Dielectric Barrier Discharges

Jun-Chieh Wang [a], Napoleon J. Leoni [b], Henryk Birecki [b], Omer Gila [b], Eric G. Hanson [b] and Mark J. Kushner [a]

(a) University of Michigan, Ann Arbor, MI 48109 USA
(mjkush@umich.edu, junchwan@umich.edu)
(b) Hewlett Packard Research Labs, Palo Alto, CA 94304 USA
(napoleon.j.leoni@hp.com, henryk.birecki@hp.com, omer_gila@hp.com, eric.hanson@hp.com)

Micro dielectric barrier discharges (mDBD's) consist of micro-plasma devices (10-100μm diameter) in which one or both of the electrodes are covered with a dielectric which seperate the electrodes from the gas. For industrial applications it is desirable for the mDBD's to be operated at atmospheric pressure driven with radio frequency (rf) wave forms. After the plasma is initiated in a mDBD, charging of the dielectric terminates the discharges by reducing the gap voltage to below its self sustaining value. When the applied voltage changes polarity, the residual dielectric charges from the previous pulse enhance the gap voltage so that a more intense electron avalanche occurs. At atmospheric pressure, and particularly in attaching gases, the plasma formation and decay times can be as short as a few to tens of ns whereas the rf period may be tens to hundreds of ns. So the micro-plasma may need to be re-ignited with each discharge pulse. In certain applications, it may be desirable to extract electron current out of the mDBD plasma. This necessitates a third electrode. As a result, the physical structure of micro-DBD, the electron emission and plasma dynamics are important to its operation.

In this presentation, we will discuss the properties of mDBD's sustained in atmospheric pressure N_2 using results from a two-dimensional plasma simulation. The micro-DBD's are sandwich structures with an opening of ten-of-microns excited with rf voltage waveforms of up to 25 MHz. The model, nonPDPSIM, solves Poisson's equation and transport equations for charge species and electron energy conservation equation for electron temperature. Rate coefficients and transport coefficients are obtained from local solutions of Boltzmann's equation for the electron energy distribution. Radiation transport is addressed using a Green's function approach. We find that plasma is avalanched by electron impact ionization in the mDBD cavity. The plasma can then be expelled from the mDBD's cavity towards the collection electrode during the part of the rf cycle when the collection electrode appears anodic. This extraction can be enhanced by biasing the extraction electrode. At lower frequencies, the plasma needs to be reformed in another part of the cycle. Long lived neutral species facilitate generating plasma by production of UV photons that continuously seed secondary electrons at surfaces until the potential is favorable to re-ignite plasma. The current extraction is a strong function of dielectric constant of dielectric barrier.

New Diagnostic Capabilities for NASA's Pulsed Nanosecond Discharge

B. T. Yee [a], J. E. Foster [a], S. J. Schneider [b], and I. M Blankson [b]

(a) University of Michigan (btyee@umich.edu)
(b) NASA Glenn Research Center

High voltage nanosecond width pulses are an interesting means of obtaining homogeneous near atmospheric discharges. While the breakdown mechanisms are believed to be similar to those of the streamers formed in dielectric barrier discharges, the repeatability of pulsed nanosecond discharges makes them preferable for in-depth study. Additionally, pulsed nanosecond discharges provide large volume ionization which has potential uses in materials processing, water and tissue sterilization, and hypersonic engines with MHD energy bypass systems.[1]

NASA Glenn Research Center has built a simple planar geometry to study the physics of such discharges.[2] Until recently, diagnostic capabilities have been limited to ICCD imaging of the plasma along with voltage and current traces. In order to reach an improved understanding of the discharge, a millimeter-wave interferometer and optical spectroscopy system have been integrated into the setup. Plans are in place for an additional optical diagnostic based on coherent anti-Stokes Raman scattering spectroscopy which would provide detailed temporal and spatial information about the electric field.[3]

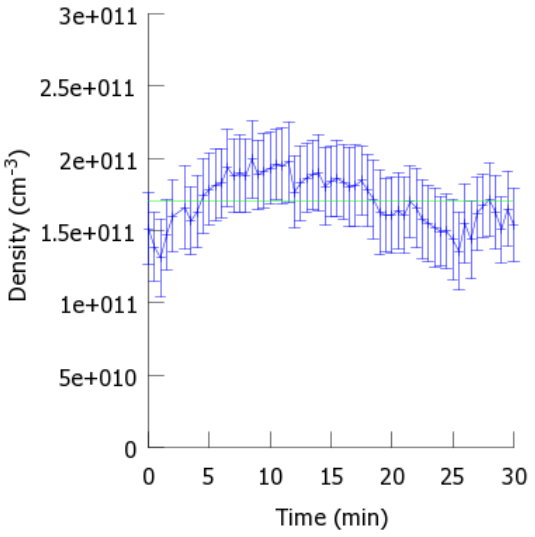

Fig. 1: Time evolution of the electron density in a pulsed nanosecond discharge with a pulse frequency of 20 kHz at 20 Torr of air.

Initial interferometer measurements of the line-averaged electron density at 75 GHz suggest a significant startup transient as seen in Figure 1. This transient lasts for approximately 7 minutes after which there is an unexplained fall in the electron density. Overall an average electron density of 1.5-3.0 x 10^{17} m^{-3} is obtained. Any difference in density between the discharge with and without the sustainer is difficult to resolve as a result of the lower than expected phase shift. An improvement in the accuracy of these results may be obtained by a reduced interferometer frequency and a better understanding of how neutral pressure transients affect the wave propagation

References

[1] I. Adamovich, W. Lempert, M. Nishihara et al., J. Prop. Pow. **24**, 1198 (2008).
[2] S. Schneider, H. Kamhawi and I. Blankson, 47th Aerosp. Sci. Mtg., AIAA-2009-1050 (2009).
[3] T. Ito, K. Kobayashi, S. Mueller et al., J. Phys. D: Appl. Phys. **42**, 092003 (2009).

Evaluation of RF Power Absorption and Electric and Magnetic Field Enhancements due to Surface Roughness

Peng Zhang, Y. Y. Lau and R. M. Gilgenbach

Department of Nuclear Engineering and Radiological Sciences
University of Michigan, Ann Arbor, MI 48109-2104

Surface roughness may lead to enhanced RF power loss on an otherwise flat surface. It may also lead to local electric field enhancement that triggers RF breakdown. In a superconducting cavity, surface roughness may cause local magnetic field enhancement that leads to quenching, i.e., rapid loss of superconductivity. In this paper, we analytically compute the power absorption due to a hemispherical protrusion on a locally flat surface. The electric field and magnetic field enhancements on the protrusion are also calculated. This protrusion may represent a foreign object since its ε, μ, and σ may take on arbitrary values.

We assume that the hemispherical protrusion has a radius a << λ, where λ is the free space wavelength of the RF electromagnetic field. This protrusion assumes an arbitrary complex dielectric constant $\varepsilon = \varepsilon_r - j\sigma/\omega$, and a real permeability μ. Associated with the electrical conductivity σ is the skin depth $\delta = [2/(\omega\mu\sigma)]^{1/2}$, which may assume any value ranging from zero (perfect conductor) to infinity (insulator).

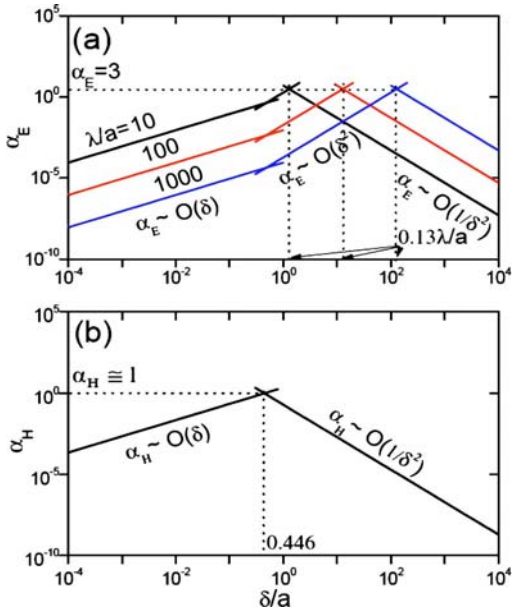

Fig. 1: The asymptotes for (a) α_E and (b) α_H as a function of δ/a for $\varepsilon_r = \varepsilon_0$, $\mu_r = \mu_0$ and various values of λ/a.

The hemispherical protrusion is situated on the locally flat surface at which, in the absence of the protrusion, the normal RF electric field is E_0 and the tangential RF magnetic field is H_0. Both E_0 and H_0 may have an arbitrary amplitude and phase. The RF power dissipated in this protrusion by E_0 and by H_0 are found to be, respectively [1],

$$P_E = \alpha_E \omega \left(1/2\varepsilon_0 E_0^2\right) V_a ,$$

$$P_M = \alpha_H \omega \left(1/2\mu_0 H_0^2\right) V_a ,$$

where $V_a = (2\pi/3)a^3$ is the volume of the protrusion, and α_E (α_H) is the particulate's electric (magnetic) polarizability, shown in Fig. 1. In Fig. 1b, α_H is independent of λ when λ/a >> 1.

We have also obtained the analytic expressions for the electric field enhancement factor and the magnetic field enhancement factor on this hemispherical protrusion [1]. These calculations have been spot-checked against the Maxwell-3D code. The δ = 0 limits also agree with those given in the literature.

References

[1] Peng Zhang, Y. Y. Lau, and R. M. Gilgenbach, "Analysis of RF absorption and electric and magnetic field enhancements due to surface roughness", J. Appl. Phys. **105**, 114908 (2009).

Electrical Contact Resistance with Dissimilar Materials

Peng Zhang and Y. Y. Lau

Department of Nuclear Engineering and Radiological Sciences
University of Michigan, Ann Arbor, MI 48109-2104

Electrical contact is important to thin film devices and integrated circuits, carbon nanotubes based cathodes and interconnects, field emitters, wire-array Z pinches, metal-insulator-vacuum junctions, and high power microwave sources, etc. Because of the surface roughness on a microscopic scale, true contact between two pieces of conductors occurs only at the asperities of the two contacting surfaces, leading to contact resistance. For a long time, the basic model for contact resistance remains that of Holm's *a*-spot [1, 2], where the current flows through a circular disk constriction of a small radius *a* and zero-thickness at the bulk interface [Fig. 1a]. Here, we vastly extend Holm's a-spot theory to high dimensions, including dissimilar materials [3].

Figure 1a shows a generalized *a*-spot (I) with a finite axial length 2*h*, joining two conducting channels (II, III). It represents a Cartesian (cylindrical) current channel with half channel width (radius) of *a*, *b* and *c* ($a \le b$, $a \le c$), and electrical resistivities ρ_1, ρ_2 and ρ_3. It is assumed that the axial extents of channels II and III are long so that the current flow is uniform far from the contact region, I. A scaling law [3] for the contact resistance has been constructed for arbitrary values of *a*, *b*, *c*, *h*, ρ_1, ρ_2 and ρ_3, for both Cartesian and cylindrical current channels. All known limiting cases are recovered from this scaling law. A sample comparison of this scaling law against the MAXWELL 3D simulation of a cylindrical channel is shown in Fig. 1b.

For the special case of $b = c$, and $\rho_1 = \rho_2 = \rho_3$, our theory recovers the models of zero-thickness constriction ($h = 0$), for both Cartesian [4] and cylindrical [2] cases. The higher dimensional theory of contact resistance was also validated by a recent experiment [5], for the special case of $\rho_1 = \rho_2 = \rho_3$, and $b = c$ of a cylindrical channel.

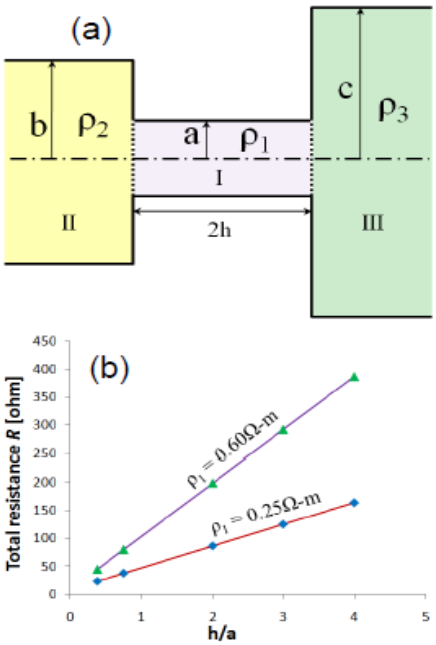

Fig. 1. (a) Cartesian (cylindrical) current channel consisting of three regions I, II, and III. Holm's *a*-spot corresponds to $h = 0$, $a << b$, $a << c$. (b) The total resistance *R* of a cylindrical channel according to MAXWELL 3D simulation (symbols) and the scaling law (solid line). In the simulation, we set $\rho_1 = 0.25$ (and 0.60)Ωm, $\rho_2 = 0.038$Ωm, $\rho_3 = 0.001$Ωm, $a = 4$mm, $b = 8$mm, $c = 10$ mm, the lengths of conductor II and III were equal, 2*h* ranging from 1.5 to 16 mm, the total axial length of the current channel simulated was fixed at 80 mm, and an excitation voltage of 10V was applied.

References

[1] R. Holm, *Electric Contact*, 4th Edition, (Springer-Verlag, Berlin, 1967).
[2] R. S. Timsit, IEEE Trans. Compon. Packag. Technol. **22**, 85 (1999).
[3] Peng Zhang, and Y. Y. Lau, J. Appl. Phys. (in the press, 2010).
[4] Y. Y. Lau and Wilkin Tang, J. Appl. Phys. **105**, 124902 (2009).
[5] M. R. Gomez *et al*., Appl. Phys. Lett. **95**, 072103 (2009).

Simulation of the Interaction between Two Rarefied Ionized Jets Using a Hybrid Method

C. Galitzine and I.D. Boyd

Department of Aerospace Engineering University of Michigan,
Ann Arbor, MI 48109
(cyrilg@umich.edu, iainboyd@umich.edu)

Accurate prediction of the shape and evolution of the velocity distribution function (vdf) is of paramount importance for the optimization of industrial processes involving low temperature plasmas (LTP) [1]. This can be readily understood by considering that the rate k of kinetic processes (such as chemical reactions) can be written as:

$$k(\vec{r},t) = \int f(\vec{v},\vec{r},t)|\vec{v}|\sigma(\vec{v})d^3\vec{v}, \qquad (1)$$

where $\sigma(\vec{v})$ is the particle cross section. This in turn implies that the rate of any such process can be maximized or minimized by optimally shaping the vdf.

The aim of this present paper is to present some preliminary simulation results obtained for a canonical flow of argon gas that was specifically crafted to study the interaction between two different species within the context of a cold ionized rarefied flow. This flow is constituted of two counterflowing jets, as shown on Fig. 1, one composed of ionized argon gas (Ar^+,e^-) and the other of neutral Ar. This canonical flow will be the subject, in upcoming years at the University of Michigan, of very detailed analyses, both experimental and numerical. Our main goal will be to validate numerical models for the prediction of the vdf for the various species in the flow.

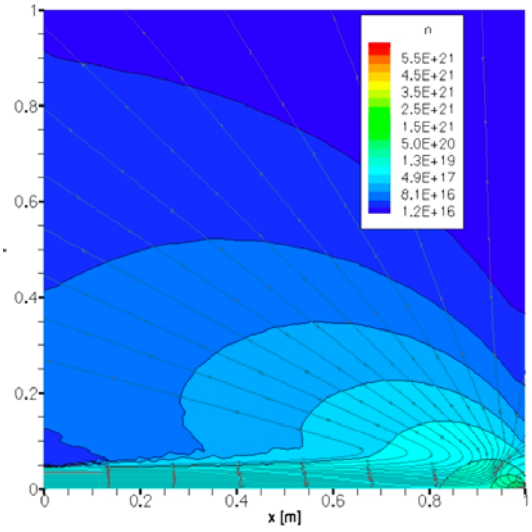

Streamline and number density n [m^{-3}]

The flow is simulated using a hybrid fluid- particle method. Collisions between heavier particles (Ar+ and Ar) are handled via a direct simulation Monte Carlo (DSMC) method [2]. A particle in cell (PIC) method [3] is used to model the effect of the electrical field on the ions. The electrical field is obtained by modeling the electrons as a fluid and making use of the Boltzmann relation [1].

An exploratory parametric study is conducted to determine the influence of the various parameters of the flow on the shape of the vdf for the heavy particles. The aim is to gain some understanding of the basic physical phenomena at play in such a flow as well as to identify any shortcomings of this simplified model that will need to be addressed in future work.

References

[1] M.A. Lieberman and A.J. Lichtenberg, Principles of Plasma Discharges and Materials Processing, Wiley-Interscience, Hoboken, 2005

[2] G.A. Bird, Gas Dynamics and the Direct Simulation of Gas Flows, Oxford University Press, Oxford, 1994

[3] C.K. Birdsall and A.B. Langdon, Plasma Physics via Computer Simulation, Adam Hilger, Bristol, 1991

Experimental and Computational Study of Carbon Dioxide Dissociation in an Atmospheric Pressure Microwave Discharge

Laura Spencer and Alec D. Gallimore

University of Michigan (laspen@umich.edu)

Rising concerns of atmospheric carbon dioxide (CO_2) concentrations has increased scientific effort to mitigate the effects of global warming. This project proposes using a plasma source to reduce CO_2 emissions by breaking down the molecule to CO and O_2 via electron impact inelastic collisions. An atmospheric pressure plasma source excited by microwaves is experimentally investigated to demonstrate the dissociation capabilities of the device. Diagnostics are taken using a residual gas analyzer to monitor the gas species present in the plasma discharge, demonstrating that CO and O_2 are the main products of dissociation. The experimental results are compared to a global, zero-dimensional kinetic model called Global_kin, which assumes a homogeneous plasma where the concentration of species is spatially independent.